Integrated Modelling for ITER in EU

V. Parail 1), P. Belo 2), P. Boerner 3), X. Bonnin 4), G. Corrigan 1), D. Coster 12), J. Ferreira 2), A. Foster 5), L. Garzotti 1), G.M.D. Hogeweij 6), W. Houlberg 7) F. Imbeaux 8), J. Johner 8), F. Kochl 9), V. Kotov 3), L. Lauro-Taroni 10), X. Litaudon 8), J. Lonnroth 11), G. Pereverzev 12), Y. Peysson 8), G. Saibene 13), R. Sartori 13), M. Schneider 8), G. Sips 12), P. Strand 14), G. Tardini 12), M. Valovic 1), S. Wiesen 3), M. Wischmeier 12), R. Zagorski 15), EFDA JET contributors[a] and EU ITM Task Force

1) EURATOM/UKAEA Fusion Association, Culham Science Centre, Abingdon OX14 3DB, United Kingdom
2) Association Euratom-IST, Lisboa, Portugal
3) Institut fur Energie Forschung-Plasma Physik,Forschungszentrum Juelich GmbH, Germany
4) LIMHP, CNRS-UPR, Université Paris 13, Villetaneuse, France
5) Dept. of Physics, Univ. of Strathclyde, Glasgow, UK
6) FOM-Institute for Plasma Physics Rijnhuizen, NL-3430 BE Nieuwegein, The Netherlands
7) ITER Organisation, 13108 St Paul lez Durance, France
8) Association Euratom-CEA, Cadarache 13108 Saint Paul LEZ DURANCE, FRANCE
9) Association EURATOM-ÖAW/ATI, Vienna, Austria
10) Consorzio RFX, Padova, Italy
11) Association EURATOM-TEKES, Helsinki University of Technology, P.O. Box 2200, FIN-02015 HUT, Finland
12) Max-Planck-Institut für Plasmaphysik, EURATOM-Assoziation, D-85748, Garching, Germany
13) FUSION FOR ENERGY Joint Undertaking, 08019 Barcelona (Spain)
14) Chalmers University, Gothenburg, Sweden
15) EFDA Close Support Unit, Garching, Germany

e-mail contact of the main author: vparail@jet.uk

Abstract. The ITER Scenario Modelling Working Group (ISM WG) is organised within the European Task Force on Integrated Tokamak Modelling (ITM-TF). The main responsibility of the WG is to advance a pan-European approach to integrated predictive modelling of ITER plasmas with the emphasis on urgent issues, identified during the ITER Design Review. Three major topics were selected, which are considered as urgent and where the WG has the best possible expertise. These include modelling of current profile control, modelling of density control and impurity control in ITER (the two last topics involve modelling of both core and SOL plasma). Different methods of heating and current drive are tested as controllers for the current profile tailoring during the current ramp up in ITER. These include Ohmic, NBI, ECRH and LHCD methods. Simulation results elucidate the available operational margins and rank different methods according to their ability to meet different requirements. A range of "ITER-relevant" plasmas from existing tokamaks were modelled. Simulations confirmed that the theory-based transport model, GLF23, reproduces the density profile reasonably well and can be used to assess ITER profiles with both pellet injection and gas puffing. In addition, simulations of the SOL plasma were launched using both H-mode and L-mode models for perpendicular transport within the edge barrier and in the SOL. Finally, an integrated approach was also used for the predictive modelling of impurity accumulation in ITER. This includes helium ash, extrinsic impurities (like argon) and impurities coming from the wall (including tungsten). The relative importance of anomalous and neo-classical pinch contributions towards impurity penetration through the edge transport barrier and further accumulation in the core was assessed.

---

[a] *See annex to M. Watkins et al, Fusion Energy 2006 (Proc. 21st IAEA Conf., Chengdu, 2006) IAEA Vienna*

1. Modelling of current profile control in ITER

Two aspects of current profile control make modelling of current ramp up/down in ITER an urgent task. First is a concern about present design of ITER PF system and its ability to ensure reliable operation of all ITER reference scenarios. Secondly, it is important to ensure that H&CD and PF systems have enough flexibility to generate any current profile and to keep it as long as it might be needed by one or the other ITER reference scenarios.

Predictive modelling of current profile evolution in ITER was done using two core transport codes Cronos [1] and Jetto [2]. Both codes have fixed boundary equilibrium solvers so they require information about evolving magnetic boundary from other codes. After that the task is reduced to a numerical solution of transport equations for toroidal current and electron and ion temperature in the plasma core with given density and Z_{eff} profiles. The following heating/current drive schemes were tested: Ohmic, ECRH, NBI, LHCD and LHH, with power and current deposition profiles calculated by internal solvers. Since both electrical conductivity (which is assumed to be neo-classical) and power and current deposition profiles for Ohmic, ECRH and LHCD depend mainly on electron temperature, the choice of the transport model for electron transport is essential. Three different transport models were used in predictive modelling of ITER scenarios, presented in this paper. First is a well-known theory-based transport model GLF23 [3]. This model being quite stiff, the temperature prediction in the core has a strong dependence on the edge plasma parameters which are not well known for L-mode plasma. We therefore use it only to simulate plasma performance during flat top burn. For the current ramp modelling, another heat transport model, a priori much less sensitive to the boundary condition, has been used. The heat diffusion coefficients are written as:

$$\chi_e = \chi_i = f \cdot (1 + 6\rho^2 + 80\rho^{20}) \qquad (1)$$

where f is dynamically adjusted during the run to keep energy confinement time as a given fraction of ITER-98(y2) confinement scaling (usually 0.4<H98y<0.5). The third model is a well-known (and tested) empirical JET Bohm/gyroBohm model [4]. Needless to say, all three models have to be tested on relevant experimental data before they are used to predict ITER plasma.

1.1 Simulation of current ramp up/down in JET

A few recent ITER-relevant JET plasmas with either Ohmic or LH-assisted current ramp up/down were selected to test transport models. Figures 1 and 2 show the result of this test for
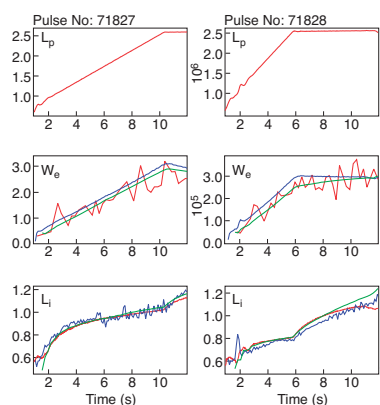

Figure 1. Time evolution of current (top), electron energy content (middle) and internal inductance (bottom): red-exp, blue-CRONOS, green-JETTO
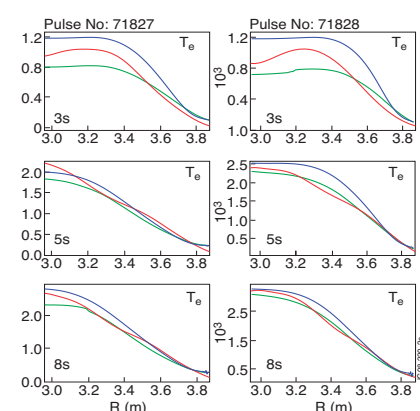

Figure 2. Electron temperature profiles at t-2, 5 and 8 sec: red-exp, blue-CRONOS, and green-JETTO

recent ITER-relevant JET plasmas with either Ohmic or LH-assisted current ramp up/down were selected to test transport models. Figures 1 and 2 show the result of this test for 2 JET Ohmic pulses with different I_p ramp rate (see [5,6]) using empirical transport model. One can conclude that both transport codes reproduce both the

current penetration (l_i time trace and q-profiles) and the heat transport (W_{the} time trace and T_e profiles) quite well with both Bohm/gyroBohm model and empirical formula (1), if we keep H98y=0.4 for L-mode. A similar conclusion can be drawn when Bohm/gyroBohm model was applied to JET current ramp down plasma, if the model is applied after the plasma returns to L-mode. It is worth noting that all above mentioned JET plasmas were considered as prototypes of ITER baseline Scenario-2 ELMy H-mode or hybrid Scenario-3 and therefore they do not require development of a non-monotonic q-profile, which is needed for steady-state plasma with internal transport barrier (ITER Scenario-4). Recently JET carried out a dedicated experiment on current ramp-up with assistance from LHCD system with P_{LH}=2MW (also about 1.5MW of NBI power was added for T_i and q-profile measurements). These well-diagnosed discharges were also used to benchmark LH ray tracing and beam tracing codes available in CRONOS and JETTO with stand-alone code LUKE [7]. As expected, simulations of current diffusion show strong sensitivity of current profile evolution with respect to electron temperature profile, LH wave spectrum and assumptions about radial broadening of the predicted LH current. Reasonable agreement between the CRONOS and JETTO codes in terms of generation of LH current was obtained (see Figure 3), although there is noticeable difference between both codes and LUKE in the position and shape of LH power and current density. Also, there is a noticeable difference in time evolution of simulated and measured l_i and loop voltage V_{loop}, which might be related to the difference in LH current profile. Note that some important macroscopic discharge characteristics (like internal inductance l_i and V_{loop}) depend not only on LH current drive but also on plasma heating due to LH waves
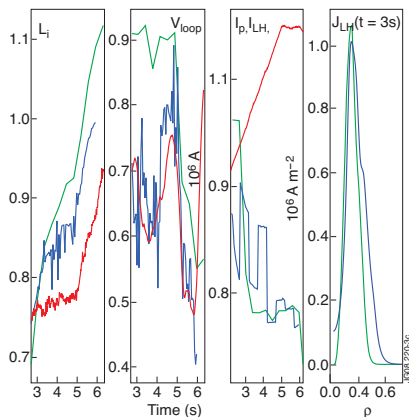

Figure 3. JET #72823, time traces of (from left to right): internal inductance, loop voltage, current and LH current profile (red-experiment, blue-CRONOS and green- JETTO

(compare with ECH heating in ITER, Figure 5). More work is needed to resolve the precise role of LH current drive and LH heating in shaping the *q*-profile in JET and ITER plasma.

1.2 Modelling of current ramp up in ITER

Two important questions to be addressed are: *(i)* how much heating power and current drive is required in ITER to reach the target q-profile for various scenarios; *(ii)* how can one minimise the flux consumption. A number of scans were done, including a density scan, a scan in magnetic configuration and scan in additional (ECRH) heating to address these issues. Very good agreement was obtained between CRONOS and JETTO in local profiles (T_e, q, j_z) and time evolving global characteristics (l_i, V_{loop}, flux consumption and W_{th}). Only the current profile and ion and electron tempera-ture profiles were predicted using scaling based transport model (1) with ion densities and *Zeff* assumed. Note that this model has been only validated against Ohmic
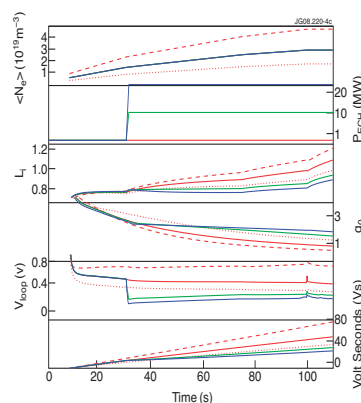

Figure 4. Effect of varying input power and density during ITER Ip ramp-up. The reference simulation (full red lines) has $<n_e>$ = 0.25 * n_G, without additional input power. Shown are simulations with 10 and 20 MW of ECRH power at mid-radius starting at 30 s, at the same density (green and blue, respectively). Also shown are simulations with $<n_e>$ = 0.15 and 0.4 * n_G without additional input power (dashed, dotted red lines, respectively). The panels from top to bottom give $<n_e>$, P_{ECRH}, l_i, $q(0)$, V_{loop} and the flux consumption.
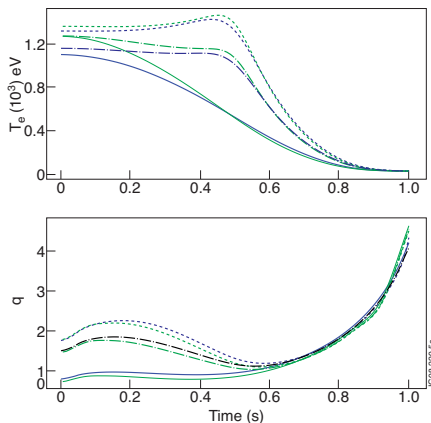
Figure 5. Final profiles of T_e (top) and q (bottom) after 100 s for the ECRH power scan of Figure 4, (solid: 0MW ECRH, chain: 10 MW, dash: 20MW; green lines – JETTO, blue- CRONOS).

current ramp up. Work is in progress to test it in cases with additional heating such as ECRH or LHCD. Note also that both fixed and evolved boundaries from [8] were used.

Figures 4 and 5 present the results of two scans: (a) a density scan from n=0.15n_G to n=0.4n_G (n_G=I_p/πa^2); (b) a scan of off-axis ECH power from 0 to 20 MW; the power is assumed to be localized at mid-radius with a narrow Gaussian deposition profile; no current drive is assumed. It is seen that the q profile at the start of the flat-top is flat with Ohmic heating, and is moderately hollow with 10 MW of off-axis ECH. The latter q profile comes close to the target profile for hybrid scenarios. Moreover, off-axis heating is crucial to keep *li* below 1 at current ramp phase. Work is in progress to assess the effectiveness of LHCD in shaping the q profile during current ramp up in ITER.

2. Predictive modelling of ITER plasma fuelling by pellets

Fully predictive simulations of ITER Scenario 2 in the H-mode phase have been carried out with JETTO and ASTRA [9] to investigate the effect of pellet injections from the high field side (HFS) on plasma performance for different assumptions regarding the outward horizontal drift of the ablated pellet material. In the plasma core, the GLF-23 model together with neo-classical transport has been used for predictive modelling of T_e, T_i, n_D and n_T (Z_{eff} profile was fixed). Transport within the ETB was emulated by an empirical continuous ELM model. Within the ETB, a constant normalised pressure gradient $\alpha_{crit.}$ = 2.0 or 2.5 (these values were confirmed by MHD stability analysis) is maintained using an empirical ELM model with the additional transport due to ELM events spread continuously over time. The transport coefficients within the ETB are calculated as follows:

$$\chi_{e,i} = \chi_{e,i\ neocl.} + C_{1,2} \cdot 10 \cdot \max\left(0, \frac{\alpha}{\alpha_{crit.}} - 1\right)^{\beta} \left[m^2/s\right],$$

$$D = D_{neocl.} + C_3 \cdot 10 \cdot \max\left(0, \frac{\alpha}{\alpha_{crit.}} - 1\right)^{\beta} \left[m^2/s\right], \quad (2)$$

with $\chi_{e,i}$ the electron or ion heat diffusivity, $\chi_{e,i\ neocl.}$ being electron or ion neo-classical diffusivity, D / $D_{neocl.}$ the respective values for particle diffusivity, C_{1-3} constant multipliers, α the maximum normalised pressure gradient within the ETB, and β an exponential parameter. The pellet source profiles were either provided by the JETTO-internal NGPS pellet model [10] or an externally coupled first-principles pellet code developed at Cadarache [11]. It could be shown that the pellet particle penetration and the fuelling efficiency strongly depend on the expected pellet drift. Simulations with transport code ASTRA were done using pellet particle source from JETTO.

These simulations address the following issues: *(i)* what will be the main ion density profile in ITER with a shallow localised particle source; *(ii)* how much plasma performance, in general (and main ion confinement in particular), depends on how deep pellets drift into plasma core; *(iii)* how much particle throughput depends on pellet penetration. It is important to stress here that since pellet ablation is very shallow, the radial distribution of ablated material and its further drift depend sensitively on plasma parameters near the separatrix (fixed in these
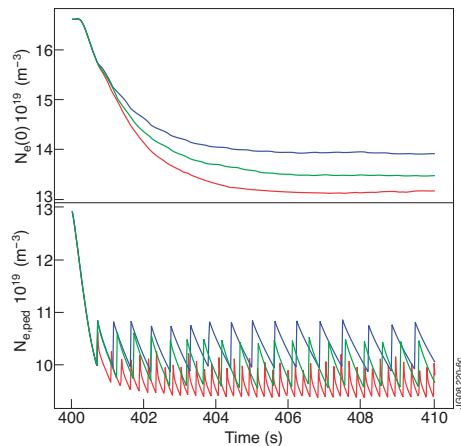
Figure 6. Axial electron density (top) and average electron density (bottom); red- 0% drift, green - 50% drift, blue - 100% drift.
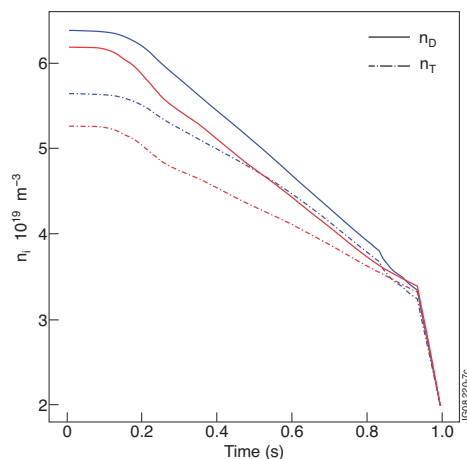

Figure 7: Deuterium density- solid (blue: 100% drift, red: 0% drift), Tritium density- dotted (blue: 100% drift, red: 0% drift)
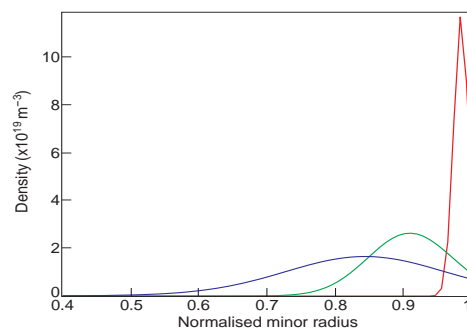

Figure 8: Source profiles for the last injected pellet in $10^{19}\ m^{-3}$, same colour code as for Figure 6.

simulations). Therefore self-consistent modelling of the SOL plasma, as well as the core plasma, is mandatory for future research.

Simulation results for 10 s runs with the model [8], applying 0%, 50% and 100% of the calculated pellet drift displacement, are shown in Figures. 6-8. Pellet composition is assumed to be 50%D and 50%T with the pellet size 5mm (cubic shape) and speed 300m/s. The average density stabilises in all cases at a constant level of $<n_e>=10^{20}\ m^{-3} \pm 5\%$ with the axial density reaching $n_e(0)=1.35 \cdot 10^{20}\ m^{-3} \pm 4\%$ (see Figure 6, note that density feedback control of pedestal density was used in these simulations). Also the average temperature remains roughly constant with time after an equilibration phase of about 2-3 seconds, although the electron temperature and energy content are reduced by 15% in the case of 100% drift mainly because of core cooling by deeply penetrating pellets. The pellet injection frequency stabilises at 5 Hz for 0%, 2 Hz for 50% and 1.5 Hz for 100% pellet drift. The energy confinement time keeps at a level of $\tau_E=1.65$ s, the average particle confinement time τ_p increases from 4 s for 0%, to 6 s for 50% and to 8 s for 100% pellet drift at $t = 410$ s. In all cases density profile is peaked with the characteristic peaking factor $n_e(0)/<n_e>=1.4$, which is expected from GLF23 model (Figure 7). Deuterium density is slightly more peaked than Tritium density due to D source from NBI. Pellet drift has little effect on density profile.

Figure 8 shows the deposition profiles of the last injected pellet for all three cases. The maxima are situated at $\rho = 0.98$, 0.91, and 0.84 for 0%, 50% and 100% pellet drift. Due to the high ablation rate already at the very edge of the ITER plasma, the pellet simulations indicate that sufficient pellet particle penetration beyond the ETB and high particle confinement times can only be reached by exploitation of the ∇B-drift for HFS injections at the available injection speeds. Comparing the 0% to the 100% drift case, the particle outflow at the edge is tripled, and the capability of the vacuum pump might reach its limit in the case of 0% drift. According to ITER IO, a fuelling rate of 100 Pa m³/s for deuterium-tritium pellets corresponds to 0.2 g/s. Following this equivalency, the average pumping capability needed in the 0%, 50% and 100% drift case can be estimated to be equal to ~ 55, 30 and 25 Pa m³/s respectively, but in the 0% drift case, the temporary particle outflow after pellet injection can increase up to > 10^{23} particles per second, corresponding to > 200 Pa m³/s. An additional potential problem with this result is that we only took into account particle

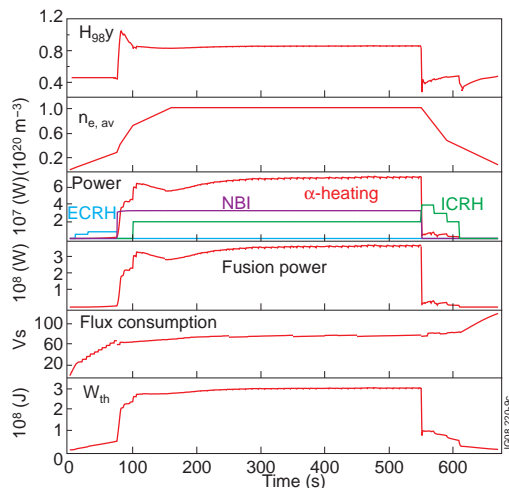Figure 9 Time traces for predictive modelling of ITER Scenario 2

outflow due to pellets. It is known that external gas puffing is needed on top of core fuelling in order to increase density near the separatrix to a level, which brings plasma to a detachment. Modelling of plasma fuelling by both methods requires self-consistent modelling of core and SOL and we will discuss some preliminary results of such modelling in Section 4. Here we would like to mention another potentially important finding, which comes from exploration of "continuous ELM" model. Our simulations show that even if contribution to particle diffusion within ETB due to continuous ELMs is equal to electron and ion thermal conductivity enhancement, its value does not exceed $D=0.1$ m^2/s to keep edge pressure gradient below the peeling/ballooning stability limit. Such low level of heat and particle transport alters conditions, needed for plasma detachment. This will be also discussed in Section 4.

Finally, a combination of scaling-based transport model (which we use during current ramp up/down phase) and "modified" GLF23 model with continuous ELMs allows full predictive modelling of ITER Scenario 2 starting from early current ramp up through steady-state burn and finishing by current ramp down. Figure 9 shows some characteristic time traces of such plasma simulations, which demonstrate that with the present knowledge of heat and particle transport it is feasible to get fusion gain Q≈10 in ITER Scenario 2 plasma.

3. Study of impurity accumulation in ITER reference scenarios

Three important questions to address in the area of impurity accumulation in ITER are considered by the Working Group: *(i)* is present ITER pumping capability adequate to remove He ash from plasma core; *(ii)* is it possible to radiate up to 70% of heat flux from the SOL by recycled impurities like Ar without the risk of plasma core contamination; *(iii)* is it possible to avoid heavy impurity (W) accumulation in the core. All three questions (particularly *(ii)* and *(iii)*)) can be adequately answered only if fully self-consistent predictive modelling of the core
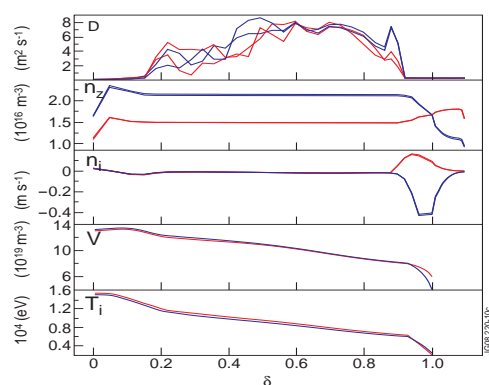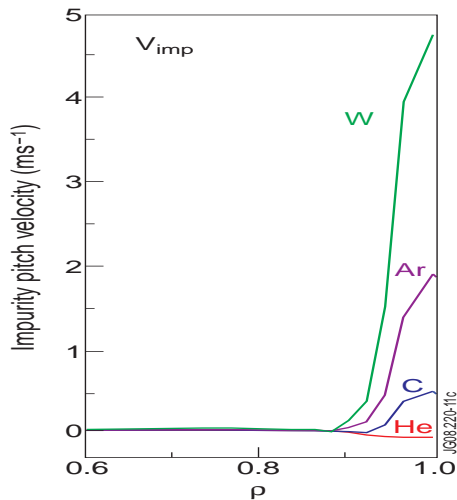

Figure 10. Radial distribution of effective Ar diffusivity: D, (solid- full description, chain line- bundled with 9 super states, red - high edge density, blue - low edge density); total Ar density: n_{Ar}, effective neo-classical pinch velocity for Ar: V_{Ar}, main ion density: n_i and ion temperature: T_i

and SOL is utilized. This is a long term program though. We will report in this paper the result of our initial investigation, which is effectively limited to a predictive modelling of impurity accumulation in plasma core, including ETB. The same transport model as in Section 2 was used in JETTO/SANCO to study impurity transport: a combination of GLF23 (for both main ions and impurity) with neo-classical transport in the core and ad hoc transport within the ETB (see (2)) to keep pressure gradient close to ballooning stability limit. It is worth noting here that the present implementation of GLF23 model for impurities (only single impurity is allowed by the model) assumes the impurity is fully ionised. This approach might be adequate for Ne or even Ar in hot ITER plasmas, but it is incorrect in case of W. Therefore our results for W should be considered

Figure 11. Neo-classical radial pinch velocity for He (red), C (blue), Ar (magenta) and W (green).

with caution. It is also worth noting that the bundled description of heavy impurities was used in these simulations, which significantly reduces the running time. Figure 10 shows the radial distribution of Ar ions in Scenario 2 ITER plasma during steady burn phase with two sets of boundary conditions for main ions. The red colour corresponds to high edge density (and low temperature), when neo-classical pinch velocity is outward directed within ETB. The blue colour relates to the opposite limiting case, when edge density is low so that the neo-classical pinch velocity is negative within ETB. Note that the same initial Ar content (uniformly distributed over the core and SOL) was used in all runs. One can observe that neo-classical pinch velocity plays a very important role in the redistribution of heavy impurities within the plasma core. The reason is that anomalous transport almost fully suppressed within the ETB (the level of ad hoc transport to keep pressure gradient below ballooning stability limit is relatively small, particularly for heavy impurities) so the sign of the neo-classical pinch controls the penetration of impurities inside edge barrier. Deeper inside, the impurity content is almost evenly distributed due to strong anomalous diffusion. Since neo-classical pinch is proportional to impurity charge Z, its role is insignificant for light impurities like N or He ash (see Figure 11). Obviously, the extremely sensitive dependence on the neo-classical impurity pinch of main ions' boundary conditions calls for fully integrated modelling of both core and SOL plasma in ITER. This will be further discussed in the next Section.

4. Predictive modelling of ITER Scenario 2 SOL plasma.

It was shown above that both main ion and impurity behaviour in plasma core are critically influenced by the conditions in the SOL. It is also true to say that SOL plasma is equally sensitive with respect to thermal and particle transport in plasma core, particularly within the ETB. Our modelling showed that if ITER manages to operate either without ELMs or with very small frequent ELMs still keeping edge pressure gradient close to peeling/ballooning limit, then the effective transport coefficient within ETB ought to fall below χ, D =0.1m^2/s. To study how the SOL plasma will react on such a small level of transport, three EDGE2D/EIRENE simulations were launched with the following assumptions about radial transport: Case 1 with "L-mode" transport $D=0.3m^2/s$, $\chi_{e,i}=1m^2/s$ in the whole simulation domain (starting from top of pedestal up to plasma wall); Case 2 with $D=0.1m^2/s$, $\chi_{e,i}=0.3m^2/s$ in the core and within 5mm outside separatrix. Transport returns to "L-mode" level further out; Case 3 with $D=0.07m^2/s$, $\chi_{e,i}=0.1m^2/s$ in the core and within 5mm outside separatrix. Transport returns to "L-mode" level further out. In all cases ion density at the separatrix is kept about $n_{sep}=4.3*10^{19}\ m^{-3}$ and total heat flux crossing separatrix P$_{sep}$=80 MW (50MW go to ions and 30MW to electrons). The main results are shown in Table 1 and Figure 12 and allow us to draw the following conclusions:

"L-mode" level of transport allows plasma to spread heat flux over a wide region in the SOL and plasma reaches full detachment on at least the inner target. This level of transport does not allow pressure gradient to reach the level close to ballooning stability limit. This translates into much reduced core plasma performance. Lower level of transport within ETB and in the near SOL recovers good performance but the price to pay is a reduced the level of plasma detachment (see Table and Figure 12, 13). It is worth noting that present maximum heat load

TABLE

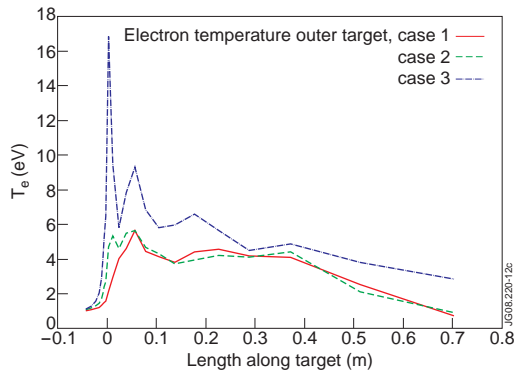|	n_{sep} 10^{19}	$T_{i,sep}$ eV	$T_{e,sep}$ eV	n_{top} 10^{19}	$T_{i,top}$ keV	$T_{e,top}$ keV	$n_{target-out}10^{21}$	$T_{i,out}$ eV	$T_{e,out}$ eV	P_{out} MW/m^2	$n_{target-in}10^{21}$	$T_{i,in}$ eV	$T_{e,in}$ eV	P_{in} MW/m^2
1	4.2	260	170	5.3	0.8	0.6	2.4	4.9	5.6	4.2	3	3.1	3.1	3
2	4.4	325	205	7	1.7	1.2	2.3	4.9	5.6	7.5	4	3.1	3.1	4.6
3	4.0	440	235	8	3	2.2	2.3	8.2	17	25	4	6.2	6.8	16

Figure 12. Electron temperature on outer target (red- "L-mode", green- intermediate quality ETB, blue- good quality ETB).
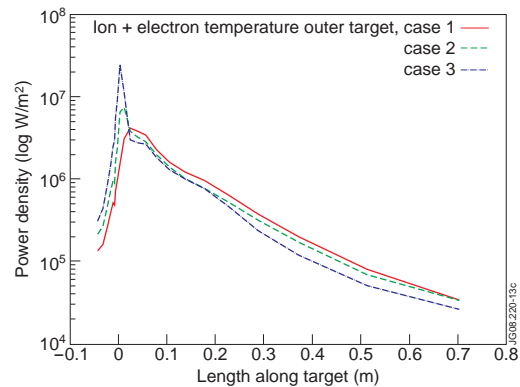

Figure 13. Total power density onto outer target (red- "L-mode", green- intermediate quality ETB, blue- good quality ETB).

near SOL recovers good performance but the price to pay is a reduced the level of plasma detachment (see Table and Figure 12, 13). It is worth noting that present maximum heat load on target plate is 10MW/m^2 and this limit is exceeded in Case 3.Although these simulations were done for a pure plasma without impurities, preliminary analysis shows that predicted temperature and density profiles near the separatrix and within ETB should not allow impurity accumulation in plasma core, particularly if ion temperature near the separatrix is kept below $T_{i,sep}$ *<300eV*. Much more modelling is required to draw any firm conclusion about possible ways to reach good core plasma parameters with a tolerable power load on the target plate in ITER reference scenarios.

References

[1] V. Basiuk et al., Nucl. Fusion **43** (2003) 822

[2] G. Cennacchi and A. Taroni, JET-IR(88) 03

[3] Waltz R.E. Phys. Plasmas **4** (1997) 2482

[4] A. Taroni et al., PPCF **36** (1994) 1629

[5] A.C.C. Sips et al., 35th Conf on Plasma Physics, Hersonissos, Crete, Greece, 2008

[6] G.M.D. Hogeweij et al., ibid

[7] Decker, J and Peysson, Y. Technical report EUR-CEA-FC-1736, December 2004

[8] C. Kessel et al., this conference IT/2-3

[9] G. V. Pereverzev et al., ASTRA : Automated System for Transport Analysis in Tokamak, Max-Planck Institutes Report, IPP 5/98

[10] L. Garzotti et al, Nucl. Fusion **17** (1997) 1167

[11] B. Pégourié et al. Nucl. Fusion 47 (2007) 44-56